FILE COPY
NO. 3

TECHNICAL MEMORANDUMS

NATIONAL ADVISORY COMMITTEE FOR AERONAUTICS

No. 751

INVESTIGATION OF BOUNDARY LAYERS ON AN AIRPLANE WING IN FREE FLIGHT

By J. Stüper

Luftfahrtforschung
Vol. XI, No. 1, May 15, 1934

THIS DOCUMENT ON LOAN FROM THE FILES OF

NATIONAL ADVISORY COMMITTEE FOR AERONAUTICS
LANGLEY MEMORIAL AERONAUTICAL LABORATORY
LANGLEY FIELD, HAMPTON, VIRGINIA

RETURN TO THE ABOVE ADDRESS.

REQUESTS FOR PUBLICATIONS SHOULD BE ADDRESSED AS FOLLOWS:

NATIONAL ADVISORY COMMITTEE FOR AERONAUTICS
1724 STREET, N.W.,
WASHINGTON 25, D.C.

Washington
August 1934

NATIONAL ADVISORY COMMITTEE FOR AERONAUTICS

TECHNICAL MEMORANDUM NO. 751

INVESTIGATION OF BOUNDARY LAYERS ON AN AIRPLANE WING IN FREE FLIGHT*

By J. Stüper

SUMMARY

This report describes the equipment and method developed for recording the boundary layers on the surface of an airfoil in free flight. The results are in close agreement with the wind-tunnel tests of other experimenters. The intensity of the turbulent boundary layer, even at the much higher Reynolds Numbers reached, is determinable with Gruschwitz's formulas, although it was impossible to definitely establish a direct relationship between the turbulent boundary layer and the Reynolds Number within the limits of the obtained accuracy. The observations on the transition from laminar to turbulent flow check with previous wind-tunnel tests and calculations.

INTRODUCTION

The investigations undertaken recently with a view to a complete mathematical solution of the characteristics of an airfoil appear very promising (reference 1). Admittedly, the potential theory affords data on the pressure distribution, and consequently the lift values which are too high compared to experiment (reference 2). But the drag, the decrease in lift due to drag, and the break-away of the flow is contingent upon the inclusion of the frictional influence on the airfoil, since the frictional phenomena occur within a layer adjacent to the wing; that is, within the so-called boundary layer. Outside of this layer the potential theory retains its validity. Several exper-

---

*"Untersuchung von Reibungsschichten am fliegenden Flugzeug." Luftfahrtforschung, May 15, 1934, pp. 26-32.

imental investigations of the boundary layer on model wings have already been made. Thus, Van der Hegge Zijnen (reference 3) explored the velocity distribution adjacent to an airfoil of 0.5 meter chord with a hot-wire anemometer; Fage and Falkner (reference 4) studied the intensity of friction on the surface of a symmetrical wing section (1.008-meter chord) with total head tubes of different types. Gruschwitz (reference 5) made measurements on an airfoil of 0.4 m chord and developed several formulas for the determination of turbulent frictional layers.

In connection with the cited investigations, it seemed very interesting to follow up the processes of the boundary layer on an airplane wing in free flight, as already attempted by Cuno (reference 6). Using ten dynamic pressure tubes which could be shifted along a wing section, he essayed to determine the velocity distribution near the wing. And while these experiments afford a picture of the trend of the boundary layer, the accuracy is, however, such as to preclude any extensive deductions.

The object of the present investigation was to obtain accurate and unquestionable data on the behavior and property of the boundary layer on the wing of an airplane in flight, to establish the transition from laminar to turbulent flow attitude, together with any eventual direct interdependence between turbulent frictional layer and Reynolds Number, and lastly, to check the conventional theoretical mathematical methods for analyzing boundary layers against the experimental data.

Test Arrangement

The airplane was a Klemm low-wing cantilever monoplane, type L 26 Va, of 13 m span, powered with a 110 horsepower Argus engine. The speed range is 90 to 165 km/h (55 to 102 m.p.h.). The experimental equipment (fig. 1) included a total-head tube a, electric motor b, worm gear c, nut d, spindle e, contact plate f, signal lamp g, guide rails h, and rubber packing i. Excepting the total-head tube a, the entire apparatus is mounted within the wing. The total-head tube is of steel with 0.7 mm outside and 0.5 mm inside diameter; the test orifice is flattened to an ellipse, whose small axis (0.3 mm inside diameter) is perpendicular to the surface of the wing. The total-head tube is controlled by electric motor b, which drives nut d over the double worm gear c. One complete revolution of d raises the spindle e one mm;

(m × 39.37 = in.) (mm × .03937 = in.)

by reversing the motor, the spindle may be lowered accordingly. The head of the spindle carries the total-head tube a. A contact plate f on the nut d gives a light signal g for every half revolution. The whole set-up slides on rails h and may be clamped at any place. The rails h were rigidly fastened to the plywood wing covering to insure constant distance between the test point of the total-head tube and the surface of the wing. Before each measurement the apparatus was moved in the desired position, the total-head tube pushed through the opening in the wing and screwed tight to the head of the spindle. The opening was sealed with a rubber gasket i, although comparative tests with and without i showed no measurable differences - probably on account of the very minute clearance (0.2 to 0.4 mm). The unused holes were plugged with plasticine. The test section was placed so as to be sheltered from the slipstream and ailerons (fig. 2). To avoid a change in profile due to aerodynamic forces, the wing was covered with plywood for a width of 1.10 m, as seen in the figure. The surface was made as smooth as possible and covered with a cloth when not used, to prevent dust from collecting on it. The electric motor and the dynamic pressure were controlled and recorded from the observer's seat (fig. 3); a shows the uneven U-tube manometers, filled with alcohol, b the Cardan suspension. The vibrations caused by the motor were damped by suitable rubber mountings. The period for setting the manometers was about 10-20 seconds. At c the total-head tube may be attached to the long or short manometer; the switches for the motor and the signal lamps are at d. The current was supplied from a 6-volt storage battery in the baggage hold.

Test Procedure

It was necessary to fly at constant dynamic pressure and at a certain altitude. The dynamic pressure was recorded with a Bruhn venturi tube. The inertia of this instrument at the beginning of the preliminary test induced oscillations about the desired dynamic pressure valve due to over-control, but an arbitrary "damping" in the control movements finally rendered a constant dynamic pressure record possible for a longer period. With increasing practice, it was then possible to raise the accuracy and constancy of the dynamic-pressure recorder to the required degree ($\pm$0.5 percent).

The momentary flight altitude was so defined that all flights were executed in constant air density ($\rho = 0.110 \frac{kg/s^2}{m^4}$). With allowance for the dependence of ρ on temperature and barometric pressure b, a value of b could be ascribed to each flight as criterion for the flight altitude. The b value was determined and maintained with a standard, but appropriately modified aneroid barometer* mounted in the pilot's cockpit. The response of this instrument to height changes made it at the same time usable as rate-of-climb meter to insure exact level flight at the desired height.

The test flights were made in perfectly still weather, very early in the morning and late in the evening. At the beginning of the experiment the measurements were repeated on the same test point until the reproducibility of the figures within the obtainable limits of accuracy had been proved. This and other similar preliminary experiments made for closer cooperation between observer and pilot, which is of paramount importance for the quality of the measurements.

The test series comprised four different speed measurements on each hole. In the suction-side experiments no visible change in the surface was observed; neither was the total-head tube bent by the aerodynamic forces. For the thicker boundary layers, a longer total-head tube was employed, reinforced in the stem and made resistent to bending by a soldered-on metal strip. The static pressure over the wing profile was determined on pressure orifices. According to experiments made there is no noticeable change of static pressure in the observer's cockpit as a result of the flow about the fuselage. Moreover, such an effect would be of no significance for the study of boundary layers because of its disappearance with the formation of differences. (See below.) The tightness of the pressure recorder was checked frequently during the experiments. Any measurement which appeared to be in the least doubtful, was repeated. To insure flight at the same c_a, it was necessary to avoid any change in the useful loading (fuel capacity, etc.).

With these precautions, no undue scatter of the velocity profiles was anticipated.

---

*Kindly supplied by the W. Lambrecht Co., Göttingen.

Evaluation of the Tests

Notation

x, development of airfoil; foremost point of profile is null point.

y, ordinate perpendicular to upper surface of wing.

u, velocity in boundary layer.

U, velocity outside of boundary layer.

U_∞, speed of airplane relative to still air.

p_o, pressure in undisturbed air stream.

q_o, dynamic pressure of undisturbed air $(= \frac{\rho}{2} U_\infty^2)$.

p, difference in static pressure relative to pressure in undisturbed air stream (in observer's cockpit).

g, difference in total head relative to pressure in undisturbed air stream (in observer's cockpit).

ϑ, height of momentum of boundary layer $(= \int_0^\delta \frac{(U-u)\,u}{U^2}\,dy)$.

η, form parameter (reference 5, etc.).

t, wing chord (= 180 cm).

ν, kinematic viscosity (≈ 0.165 cm^2/s).

c_a, lift coefficient of airfoil at point of test section.

q, dynamic pressure outside of boundary layer $(= \frac{\rho}{2} U^2)$.

g_1, difference in total head at point $y = \vartheta$ relative to pressure in the undisturbed air stream.

The test program included four series I, II, III, and IV at 100, 120, 140, and 160 km/h speeds. The venturi tube and the indicating instrument were calibrated in the wind tunnel to obtain the true speeds U_∞ for these series of measurements. The wing-flow effect on the recording of the instrument was allowed for (reference 6). The final results are appended in table I.

(cm × .3937 = in.) (cm^2/s × .1550 = sq.in./sec.)
(km/h × .62137 = mi./hr.)

TABLE I

Test series	U_∞		$\frac{U_\infty t}{\nu}$	c_a	q_o
	km/h	m/s	10^6		kg/m^2
I	96.6	26.84	2.82	0.91	39.6
II	118.2	33.2	3.62	0.55	60.7
III	140.5	39.0	4.26	0.40	83.8
IV	161.0	44.7	4.88	0.31	110.0

The value of g was determined with the venturi tube. It changes to q_o outside of the boundary layer. The fact that the dynamic pressure q_o in a test series is the same at any point outside of the boundary layer is an advantage. The limit of the boundary layer, rather than being indicated by g when it becomes constant, is exactly shown with the reaching of the value q_o, which is known for every test series.

The relation is: $$\frac{\rho}{2} u^2 + p = g$$

and with $$\frac{\rho}{2} U_\infty^2 = q_o$$

the velocity distribution in the boundary layer becomes:

$$\frac{u}{U_\infty} = \sqrt{\frac{g - p}{q_o}}.$$

The values of g, p, and q_o are known from the measurements. The course of the static pressure p/q_o across the wing section is shown in figure 4. The comparatively smooth pressure justifies the assumption that the aerodynamic forces have not disturbed the contour of the airfoil. The recorded velocity profiles of the boundary layer are illustrated in figures 5, 6, 7, and 8. Upwardly the velocity u, made nondimensional by the flight speed U_∞, is plotted against the y ordinate, which is normal to the surface of the airfoil. The first profiles on the suction side are laminar, followed by transition to the typical turbulent velocity profiles. The first profile in the test series II, III, and IV is laminar in the pressure-side measurements. In series I, this test orifice did not afford sufficient accuracy, due probably to the nearness of the stagnation point.

(m/s × 3.28083 = ft./sec.) (kg/m^2 × .204818 = lb./sq.ft.)

The Laminar Turbulent Transition

The transition point at the suction side is in very close agreement with the wind-tunnel experiments (references 3, 4, and 5). The transition occurs at about 0.1 to 0.3 t from the leading edge of the airfoil. The assumption that turbulence starts in direct proximity of the nose of the wing (reference 8), holds only for very rough estimation. This fact should under no circumstances be ignored in the analysis of the boundary-layer effect on the wing characteristics. The measurements are also compatible with the hitherto numerical-theoretical investigations on the transition point. The Reynolds Numbers of the transition $\left(R = \frac{U(x)\,\vartheta(x)}{\nu}\right)$ (reference 1a) lie in the range given by Gruschwitz (reference 9) between 250 and 650. The transition point changes very little from one test series to the next. A smaller angle of attack would shift it to the rear, whereas the higher Reynolds Number $(U_\infty t/\nu)$ shifts it forward. In the test series with increasing velocity the transition point shifts slightly forward.

The point of transition on the pressure side was unfortunately not accurately determinable because the location of the front spar did not permit suitable shifting of the apparatus. However, the records for the pressure side do show that at the usual angles of attack the transition occurs sooner than on the suction side.

An extensive investigation on the mechanism of laminar turbulent transition, its dependence on the pressure and the Reynolds Number is under way, in which the present data are to be utilized.

Comparison between Measurement and Analysis

It seemed of interest to compare these test data with Gruschwitz's formulas for turbulent boundary layers (reference 5). He used two parameters: ϑ, a criterion for the boundary-layer thickness, and η, a criterion for the profile form. From momentum theory and experiments, he evolved two differential equations which afford ϑ and η for a given pressure and an initial value of ϑ. H. Schmidbauer (unpublished report) explored the effect of the curvature. However, the effect may be ignored in this comparison, as in the present measurements the profile portions

along which the flow is turbulent, are sufficiently flat.

For comparison, we analyzed the pressure record mathematically, the initial ϑ values also being taken from the records. The result is shown in figure 9. The open rings are the measured η values, the dots the measured ϑ values. The solid-line curves are defined conformably to Gruschwitz's method (reference 5). The accord between the recorded points and the computed curves is mutually compatible with the exception of the last two test points on the suction side, and the last one on the pressure side. For lack of space, the test apparatus had to be mounted on the outside (fig. 10). Despite the faired housing B, this protuberance produced a dead air space which, with pressure changes, gains in effect on the boundary layer (split-flap effect).

Effect of Reynolds Number on the Turbulent Boundary Layer

Indirectly, the Reynolds Number has a profound effect on the transition from laminar to turbulent flow and through it on the boundary layer. Gruschwitz found no definite direct effect in his measurements. He plotted

$$\frac{\vartheta}{q}\frac{d\,g_1}{dx}$$

against the profile parameter η and obtained the straight line of figure 11. The dots are determined from the present measurements. The corresponding Reynolds Numbers $\left(R = \frac{U(x)\,\vartheta(x)}{\nu}\right)$ are given in table II.

The inaccurate measurements near the trailing edge were ignored. There is no systematic scatter according to Reynolds Numbers. But according to Nikuradse's very precise and extensive measurements of turbulent flows in water (reference 10), there is, even if only slight, a direct effect of the Reynolds Number on the turbulent boundary layer. Still, it seems that in measurements in air (cf. Gruschwitz, Stuper) this process is overshadowed by other effects (change in degree of roughness, in the nature of the flowing air stream, etc.). Figure 11 shows the present measurements to compare very favorably with the hitherto experimental results. The greater scatter is due to the greater difficulty in removing sources of error in free flight than in wind-tunnel experiments.

TABLE II

Test series I			Test series II		
η	$\frac{\vartheta}{q}\frac{dg_1}{dx}$	R	η	$\frac{\vartheta}{q}\frac{dg_1}{dx}$	R
0.519	0.00004	1325	0.556	0.00041	1074
0.546	0.00026	2637	0.550	0.00027	2921
0.581	0.00058	4180	0.570	0.00056	4773
0.528	0.00013	461	0.569	0.00040	1274
0.511	-0.00006	1054	0.537	0.00021	1495
0.530	0.00000	1170	0.510	0.00002	1838
0.500	-0.00010	1800	0.526	0.00000	2780
0.482	-0.00008	2261	0.531	0.00013	3205
Test series III			Test series IV		
η	$\frac{\vartheta}{q}\frac{dg_1}{dx}$	R	η	$\frac{\vartheta}{q}\frac{dg_1}{dx}$	R
0.539	0.00017	916	0.550	0.00033	3710
0.547	0.00038	3240	0.570	0.00047	5510
0.569	0.00055	4978	0.604	0.00088	8650
0.610	0.00096	8410	0.599	0.00103	10120
0.546	0.00038	1720	0.570	0.00051	2318
0.535	0.00022	2175	0.541	0.00026	3460
0.540	0.00017	2820	0.545	0.00024	3960
0.534	0.00020	4014	0.545	0.00025	4925
0.530	0.00021	4535	0.542	0.00026	6051

Translation by J. Vanier,
National Advisory Committee
for Aeronautics.

REFERENCES

1. Betz, A.: Theoretische Berechnung von Tragflügelprofilen. Z.F.M., August 28, 1933, p. 437.

1a. Stüper, J.: Auftriebsverminderung eines Flügels durch seinen Widerstand. Z.F.M., August 28, 1933, p. 439.

2. Betz, A.: Untersuchung einer Joukowskyschen Tragfläche. Z.F.M., Dec. 24, 1915, p. 173.

3. Van der Hegge Zijnen, B. G.: Some Experiments on the Distribution of Velocity, Pressure and Total-Head in the Neighborhood of an Aerofoil for Two-Dimensional Flow. Comptes Rendus du IV^{e} congrès international de la navigation aérienne, Rome, 1928, p. 5.

4. Fage, A., and Falkner, V. M.: An Experimental Determination of the Intensity of Friction on the Surface of an Aerofoil. R. & M. No. 1315, British A.R.C., 1930.

5. Gruschwitz, E.: Die turbulente Reibungsschicht in ebener Stromung bei Druckabfall und Druckanstieg. Ing.-Arch. 2, 1931, p. 321.

6. Cuno, O.: Experimental Determination of the Thickness of the Boundary Layer Along a Wing Section. T.M. No. 679, N.A.C.A., 1932.

7. Repenthin, W.: Investigation of the Variations in the Velocity of the Air Flow about a Wing Profile. T.M. No. 575, N.A.C.A., 1930.

8. Müller, H.: Der Reibungswiderstand umströmter Körper. Werft-Reederei-Hafen 13, 1932, p. 54.

9. Gruschwitz, E.: The Process of Separation in the Turbulent Friction Layer. T.M. No. 699, N.A.C.A., 1933.

10. Prandtl-Betz: Ergebnisse der Aerodynamischen Versuchsanstalt zu Gottingen, vol. IV, 1932, p. 18.

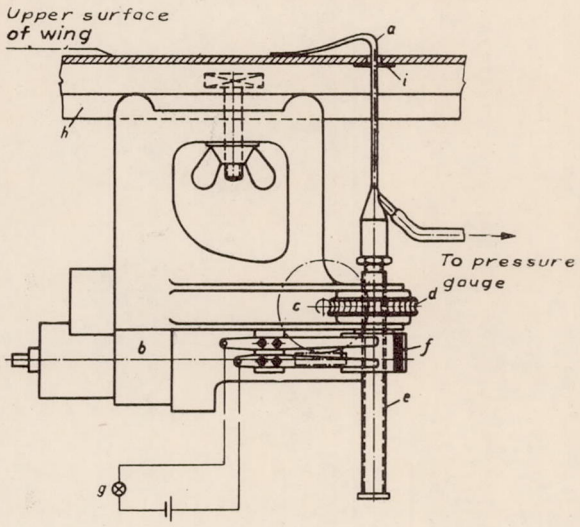

Figure 1.- Test apparatus.

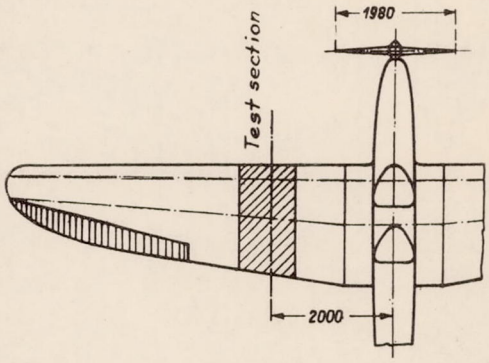

Figure 2.- Location of test section.

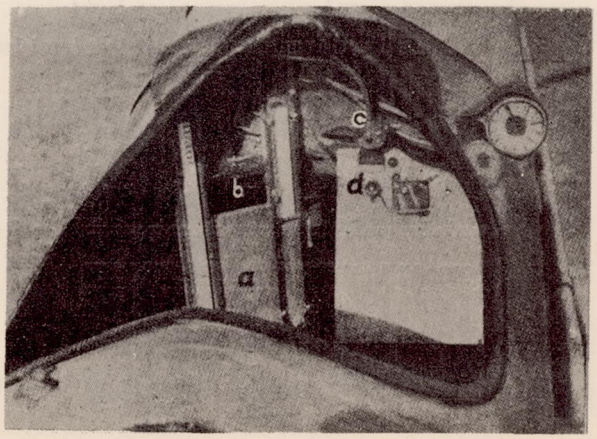

Figure 3.- Observer's cockpit.

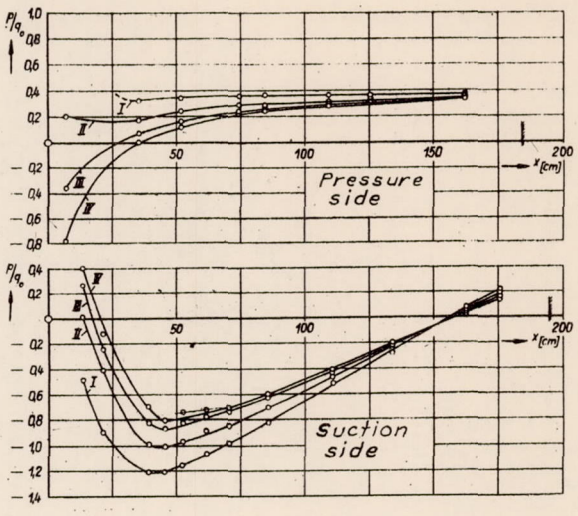

Figure 4.-Pressure distribution across the test section.

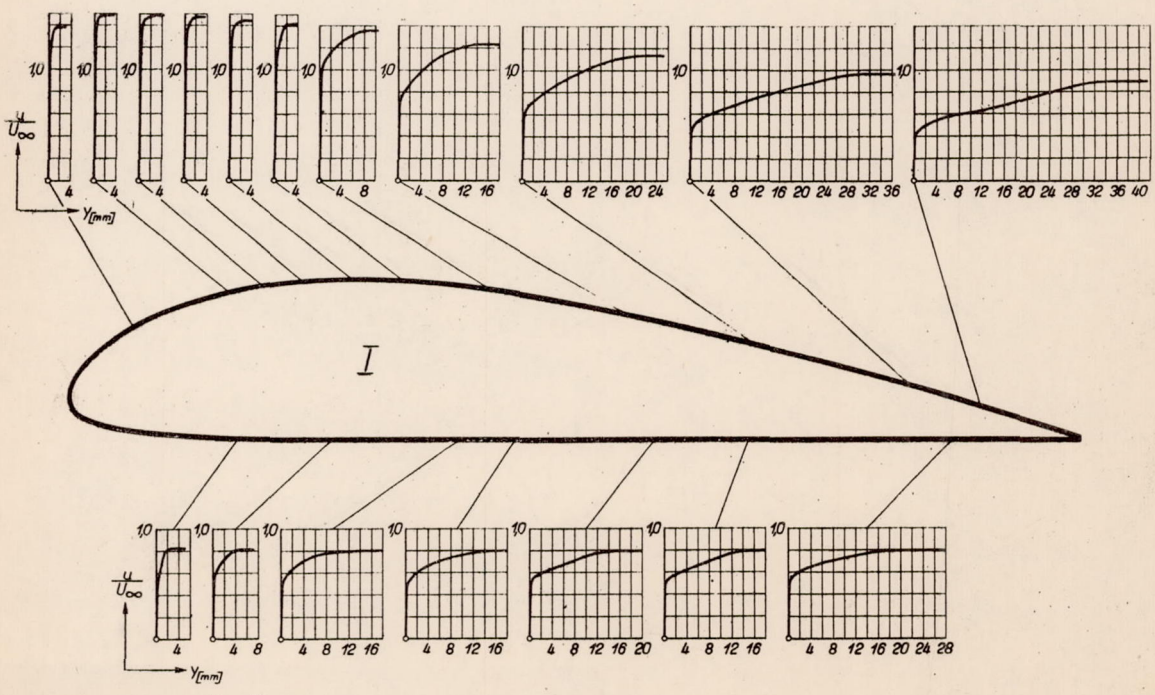

Figure 5.-Velocity profiles, test series I.

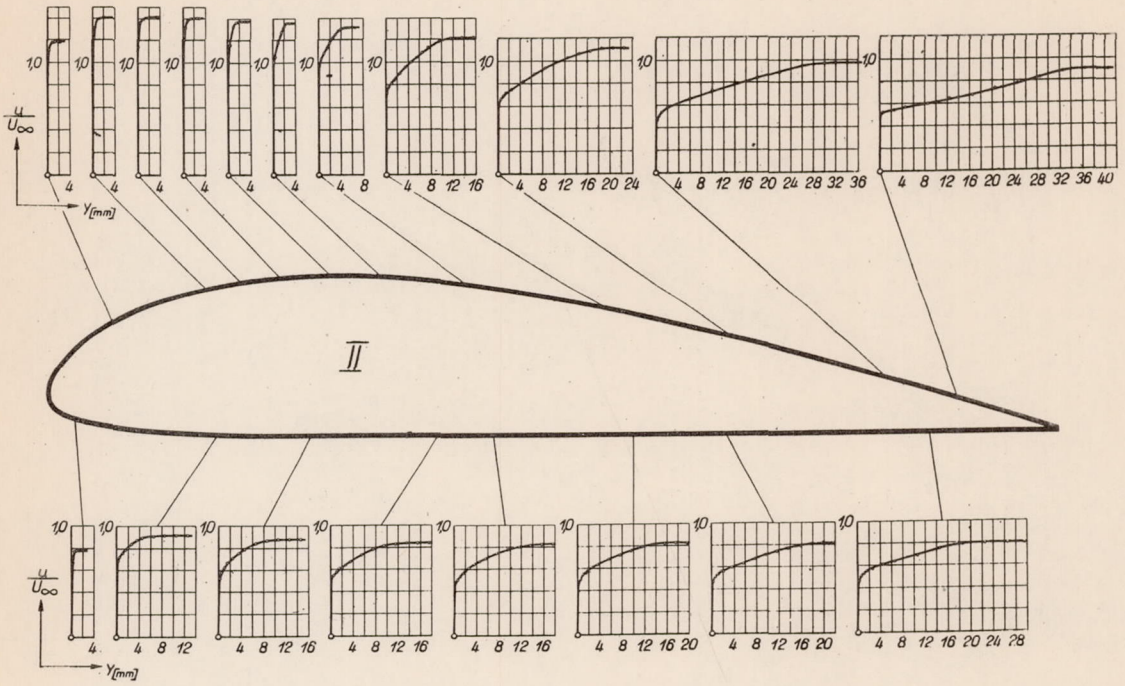

Figure 6.-Velocity profiles, test series II.

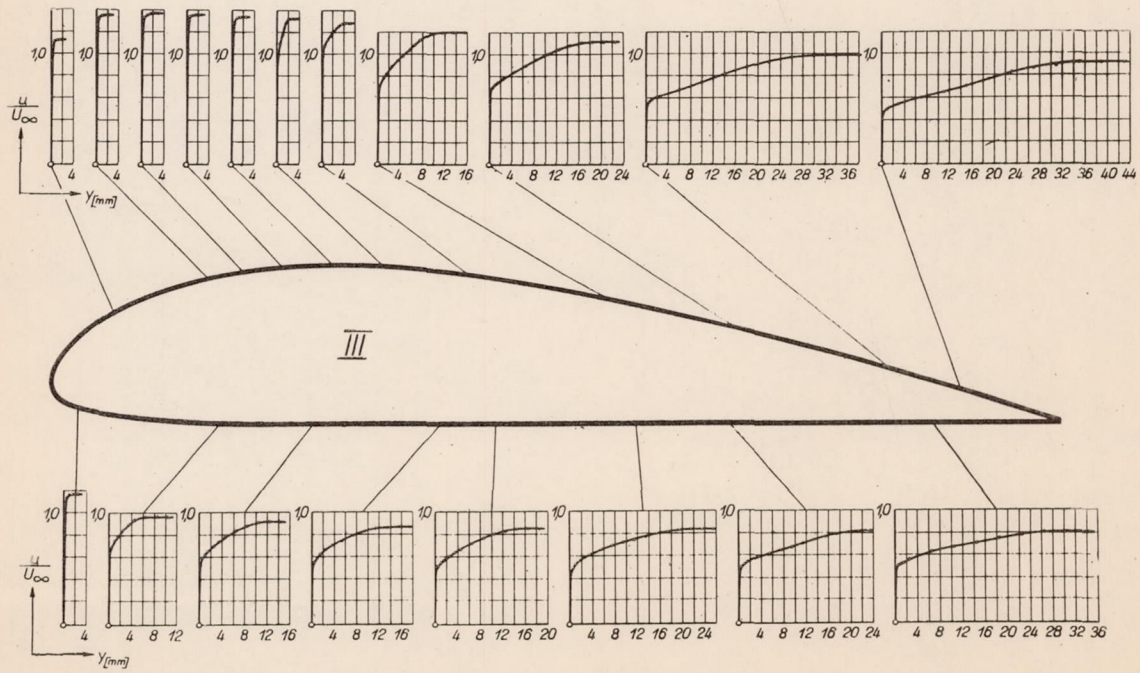

Figure 7.-Velocity profiles, test series III.

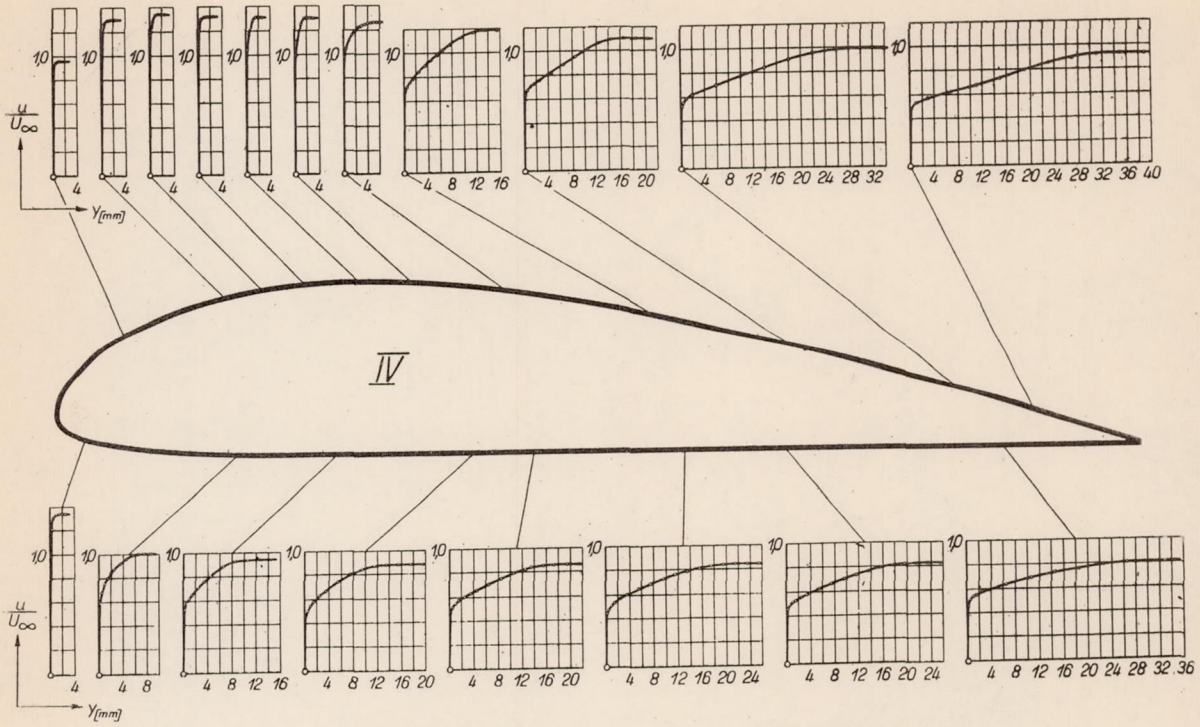

Figure 8.-Velocity profiles, test series IV.

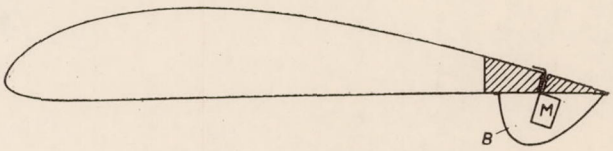

Figure 10-Installation at suction side near trailing edge.

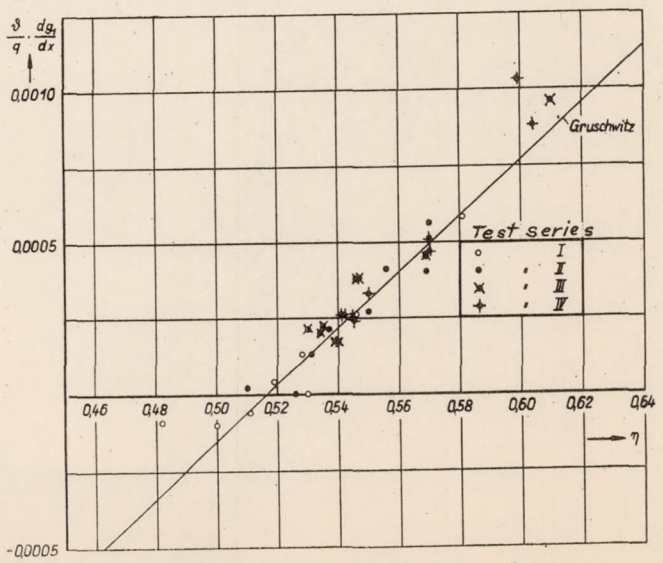

Figure 11.

Test series I

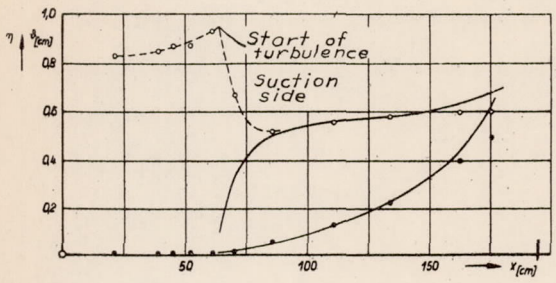

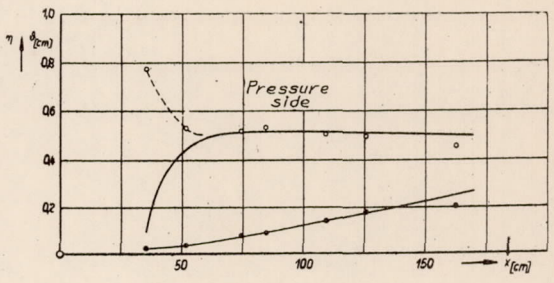

Test series II

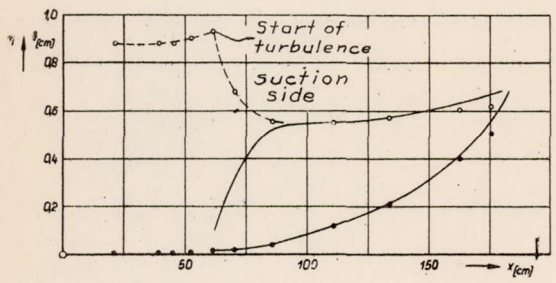

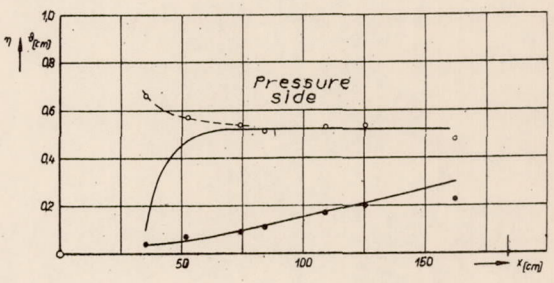

Test series III

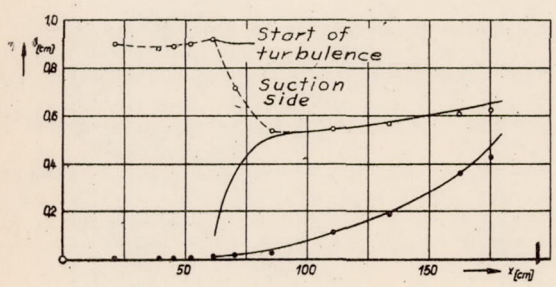

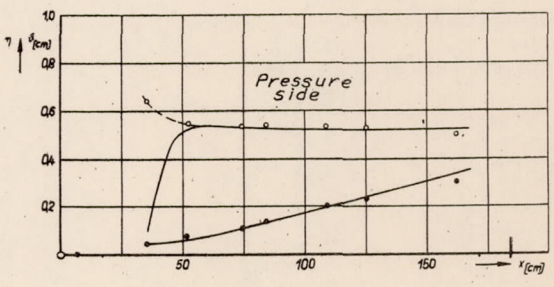

Test series IV

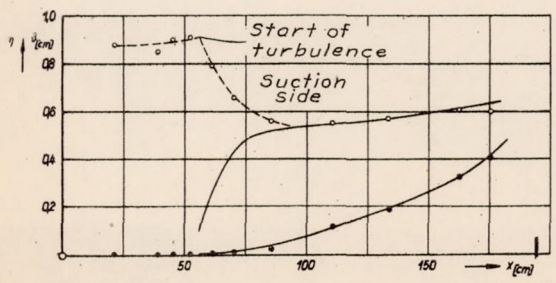

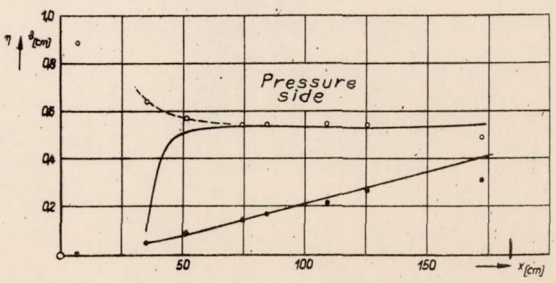

Figure 9.-Comparison between measurement and calculation.